LAWRENCE
LIVERMORE
NATIONAL
LABORATORY

LLNL-TR-420208

Simulation of Seismic Waves from Underground Explosions in Geologic Media: FY2009 Progress Report

A. Rodgers, O. Vorobiev, B. Sjogreen, N. A. Petersson

November 13, 2009

Disclaimer

This work performed under the auspices of the U.S. Department of Energy by Lawrence Livermore National Laboratory under Contract DE-AC52-07NA27344.

Simulation of Seismic Waves from Underground Explosions in Geologic Media: FY2009 Progress Report

Arthur Rodgers, Oleg Vorobiev, Bjorn Sjogreen and Anders Petersson
Geophysical Monitoring Program, Lawrence Livermore National Laboratory
Livermore, CA 94551
Email: rodgers7@llnl.gov Phone: 925-423-5018

Abstract

This report summarizes work done after one year on project LL09-Sim-NDD-02 entitled "Exploratory Research: Advanced Simulation of Low Yield Underground Nuclear Explosions To Improve Seismic Yield Estimation and Source Identification". Work on this effort proceeded in two thrusts: 1) parametric studies of underground explosion generated motions with GEODYN; and 2) coupling of GEODYN to WPP. GEODYN is a code for modeling hydrodynamic (shock-wave) motions in a wide variety of materials, including earth materials. WPP is an anelastic finite difference code for modeling seismic motions. The sensitivity of seismic motions to emplacement conditions was investigated with a series of parametric studies of low-yield (0.2-4 kiloton) chemical high-explosive shots at a range of burial depths in four canonical geologic media (granite, limestone, tuff and alluvium). Results indicate that the material has a strong impact on the seismic motions consistent with previous reports. Motions computed with GEODYN in realistically complex material models are very consistent with reported motions from nuclear tests by Perret and Bass (1975). The amplitude, frequency content and cavity size resulting from explosions are all strongly sensitive to the material strength. Explosions in high-strength (granite) resulted in the highest amplitude, shortest duration pulse and smallest cavities, whereas explosions in low-strength material (alluvium) resulted in the lowest amplitudes, longest duration pulse and larger cavities. The corner frequencies of P-wave motions at take-off angles corresponding to propagation to teleseismic distances show corresponding behavior, with high-strength materials having the highest corner frequency and low-strength materials having low corner frequency. Gravity has an important effect on the cavity size and outgoing motions due work done against lithostatic stress. In fact without gravity the cavity radius and elastic motions are largely insensitive to depth of burial. We investigated the effects of depth of burial for a given yield and material model in the presence of gravity and found that the cavity radius is slightly smaller for deeper shots and the resulting motions have shorter duration and higher corner frequency compared to shallower shots. On the second thrust, progress has been made on one-way coupling of GEODYN to WPP. Early in the project we demonstrated this capability from one-dimensional (1D) GEODYN calculations. We have now completed the capability to pass motions computed in 2D or 3D with GEODYN to WPP and propagated (in 3D) to large distances.

Introduction

Large underground nuclear explosions (UNE's) in earth materials generate shock waves that ultimately propagate to long-ranges as seismic waves. Understanding the generation

of seismic waves by UNE's is fundamental to nuclear explosion monitoring and can improve estimates of source properties by removing systematic effects in seismic observables such as amplitude, frequency content and P-to-S-wave partitioning. It has long been known that near UNE's, the material in the source region undergoes dramatic irreversible processes including the vaporization of rock, formation of a cavity, fracture, plastic deformation (including porous compaction), spall and cavity collapse. Figure 1a shows an idealized illustration of the near-source region of a UNE showing the cavity, fracture, plastic and spall regions. In the simplest case the cavity, fracturing and plastic zones can be considered spherically symmetric as is depicted in Figure 1a. The radii of these zones are known to increase with yield and have been approximated to be multiplicative factors of the cavity size. For a UNE of yield W, given in kilotons, Lamb (1988) reports the cavity radius, R_c is approximated as 14 $W^{1/3}$ meters, and the radius to the fracture, R_f, and plastic zones, R_p, are 3 R_c and 5 R_c, respectively (shown in Figure 1b). The radius where plastic deformation ends is often referred to as the elastic radius. Knowing the elastic motions on a (possibly non-spherical) surface encompassing the elastic radius would in principle allow complete description of the subsequent seismic wave propagation via the uniqueness theorem (Aki and Richards, 1980).

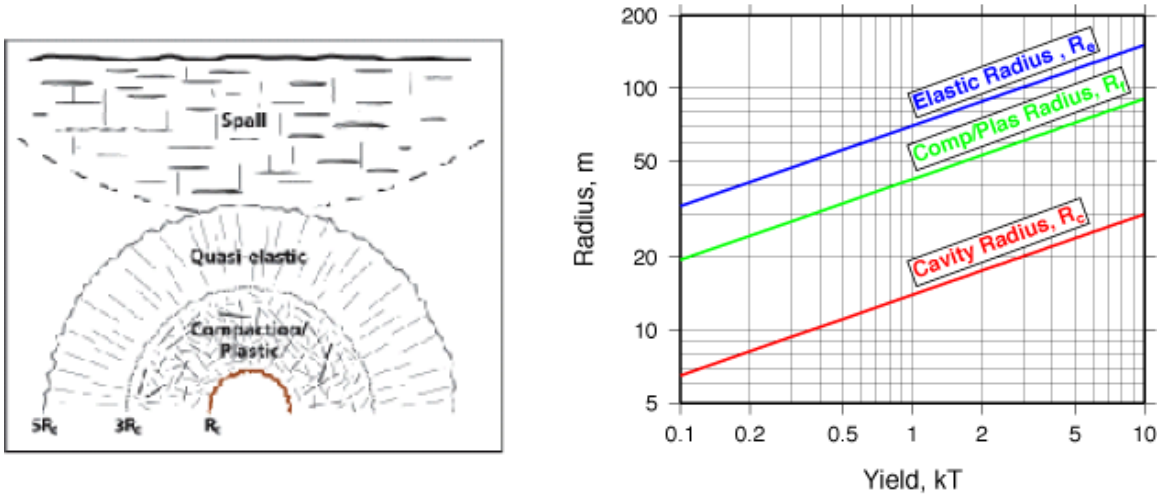

Figure 1. ***(a)*** *Schematic of the post-event near-source region of an underground nuclear explosion (UNE) showing the cavity, plastic deformation and spall regions.* ***(b)*** *Approximate sizes of the cavity, plastic and elastic radius as a function of yield for fully-coupled UNE's (Lamb, 1988).*

It is well established from experimental data that the amplitudes and frequency content of seismic waves generated by nuclear explosions are strongly dependent on the emplacement depth and lithology - especially important are material properties such as density, strength (rigidity) and porosity (e.g. Werth and Herbst, 1963; Murphy, 1981; Rodean, 1981). Perhaps the best-known example of emplacement condition effects is the variation in magnitude-yield relationships with different nuclear test site locations. For example, relationships between body-wave magnitude and explosive yield have been reported by Murphy (1981, 1996).

Many studies have sought to describe the source-time function for nuclear explosions including the variation with yield, depth of burial and emplacement conditions (see for example studies by Sharpe, 1942; Mueller and Murphy, 1971; Helmberger and Hadley, 1981; Denny and Johnson, 1991; Saikia et al., 2001). These studies are based on a theoretical description of an idealized explosion (e.g. usually a pressure pulse acting at the spherically symmetric elastic radius in an elastic whole-space) and in some cases parameters have been estimated from UNE ground motion data. Walter et al. (1995) reported differences in high-frequency P/S ratio discriminants for explosions conducted in materials of different material strengths, using gas porosity as an analog to strength. Specifically, explosions in high-strength materials generate stronger high frequency P-wave than explosions of approximately the same size and depth conditions. This results in different behavior of earthquake-explosion discriminants, such as high frequency P-wave to low frequency S-wave energy (e.g. Pn 6-8 Hz/2-4 Hz Lg).

The objective of this project is to develop a capability to simulate underground nuclear explosions (UNE's) through a series of first-principles simulations including hydrodynamic and elastic scattering effects near the explosion. This capability will be applied to better understand source emplacement conditions and their effect on seismic yield and source identification estimates, ultimately reducing uncertainties. In this study we are concerned with seismic motions excited by fully coupled and contained underground explosions where the explosive device is in full contact with the surrounding medium and placed in the Earth at a depth of burial (DOB) sufficient to prevent release of explosive reaction products or radiation in the case of UNE's. We seek to improve understanding of the amplitudes and frequency content of seismic wave generated by explosions in different emplacement conditions (e.g. geologic media, depth of burial). We apply modern numerical simulation methods, which capture much of the physics of shock-wave propagation, validated material models and high-performance computing to the task of understanding the seismic wave generation. The methods and models are verified and validated to establish the validity of the approach, but this is limited to available empirical data. While further verification and validation will be challenging, but required to improve fidelity of simulation predictions, this study establishes that physics-based (i.e. first principles) predictions of seismic ground motions are possible and promise improve prediction of seismic observables to reduce scatter in yield estimates and discriminants measures and to compute explosion scenarios for testing seismic monitoring methods.

Shock-Wave Simulations

Simulation Configuration

Numerical simulations of explosions were performed with GEODYN, an Godunov based Euleran code with adaptive mesh refinement capability. This code simulates the motions excited by high-energy density explosions and impacts in Earth materials including shock-waves, cavity formation, porous compaction and damage (Antoun et al., 2001, 2004; Antoun and Lomov, 2003; Lomov et al., 2003). GEODYN includes the effects of porosity and elastic-viscoelastic response including tensile as well as compressional

failure (Rubin et al., 2000; Vorobiev, 2008). This is important for including the effect of the rarefaction wave generated by reflection of the compressional wave by the free surface.

Simulations were performed in an axi-symmetric two-dimensional geometry. GEODYN uses a Cartesian mesh with an adaptive mesh refinement scheme to track the shock-wave. To capture the initial spreading of the shock, we used a finer mesh around the explosion emplacement superimposed on coarser mesh. The dimensions of the domain were 3000 m and 1500 m in the horizontal and vertical directions, respectively. The fine and coarse mesh had grid spacings of 0.30 and 1.25 meters, respectively. The source was placed at depth below the origin and the motions were output at marker points distributed radially outward from the source. In all cases sources are modeled as chemical explosions.

At each marker point we output the velocities and stresses and other material and physical properties. The material properties in the solid earth were considered constant with the exception of lithostatic pressure and stress (discussed below). GEODYN can output the strain at any time step in the calculation, allowing us to determine if the material is undergoing finite motions related cavity formation, plastic, infinitesimal (elastic) deformation or anything in between. We will use this feature to quantitatively evaluate the behavior shown in Figure 1. Figure 2 shows the simulation configuration and marker point locations.

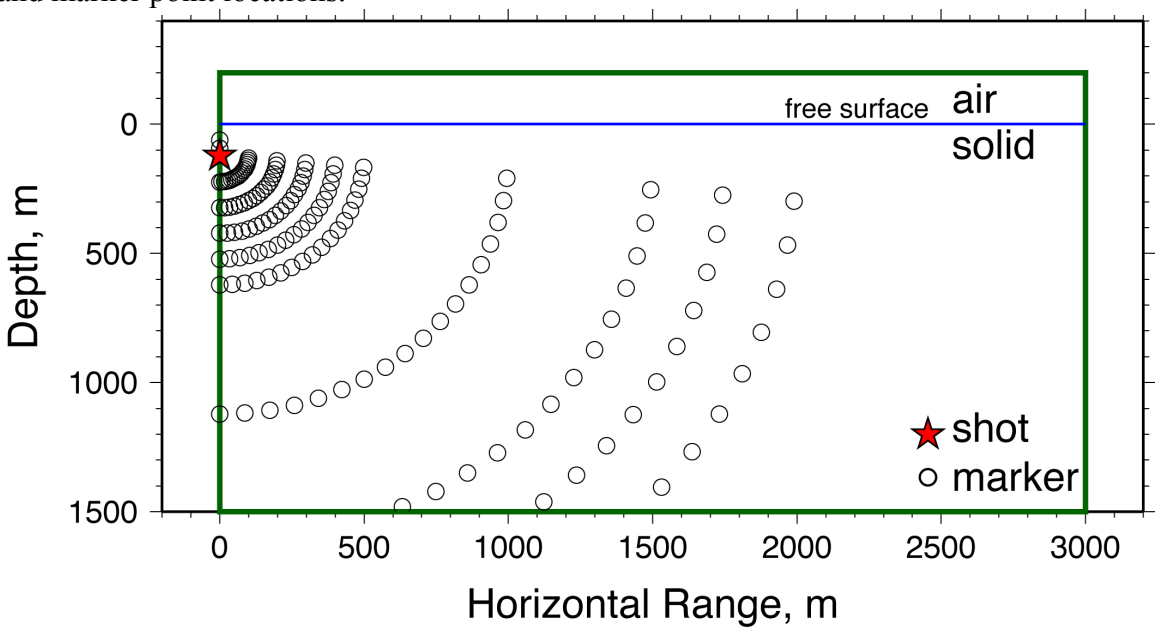

Figure 2. *Configuration of 2D axisymmetric GEODYN simulations used in this study. The source (star) was placed at depth below the origin and motions were output at marker points (circles).*

The models included air as a low-density gas over the solid Earth. Gravity is included in the modeling by introducing a lithostatic pre-stress equal to ρgz, where ρ is the density, g is gravitational acceleration (9.8 m/s) and z is the depth from the free-surface. For simplicity we assumed the materials had constant material properties (Table 1). Future

improvements could relax this assumption and model depth- or range-varying material as homogeneous layers (e.g material discontinuities, scatters, faults). Marker points were introduced to sample and output the transient wavefield at equidistant points from the source (Figure 2).

Material Properties and Validation

Underground explosions in the earth generate shock waves that load geologic materials well beyond their linear elastic behavior. Seismic wave propagation assumes elastic behavior with weak anelasticity and requires the density (r), compressional and shear wave speeds (v_P and v_S, respectively) and quality factors (Q_P and Q_S, respectively). Shock wave modeling requires characterization of non-linear material properties such as yield strength, porosity and other parameters, all of which may depend on stress and/or strain. In this study we considered four canonical materials known to have different wave propagation properties: granite, tuff, limestone and alluvium. We chose these materials because we have material models and experimental data from previous work and for their variability in material behavior. Figure 3 shows the uniaxial stress versus uniaxial strain and equivalent elastic behavior for three materials and indicates that they behave very differently to loading. Material properties are compiled in Table 1.

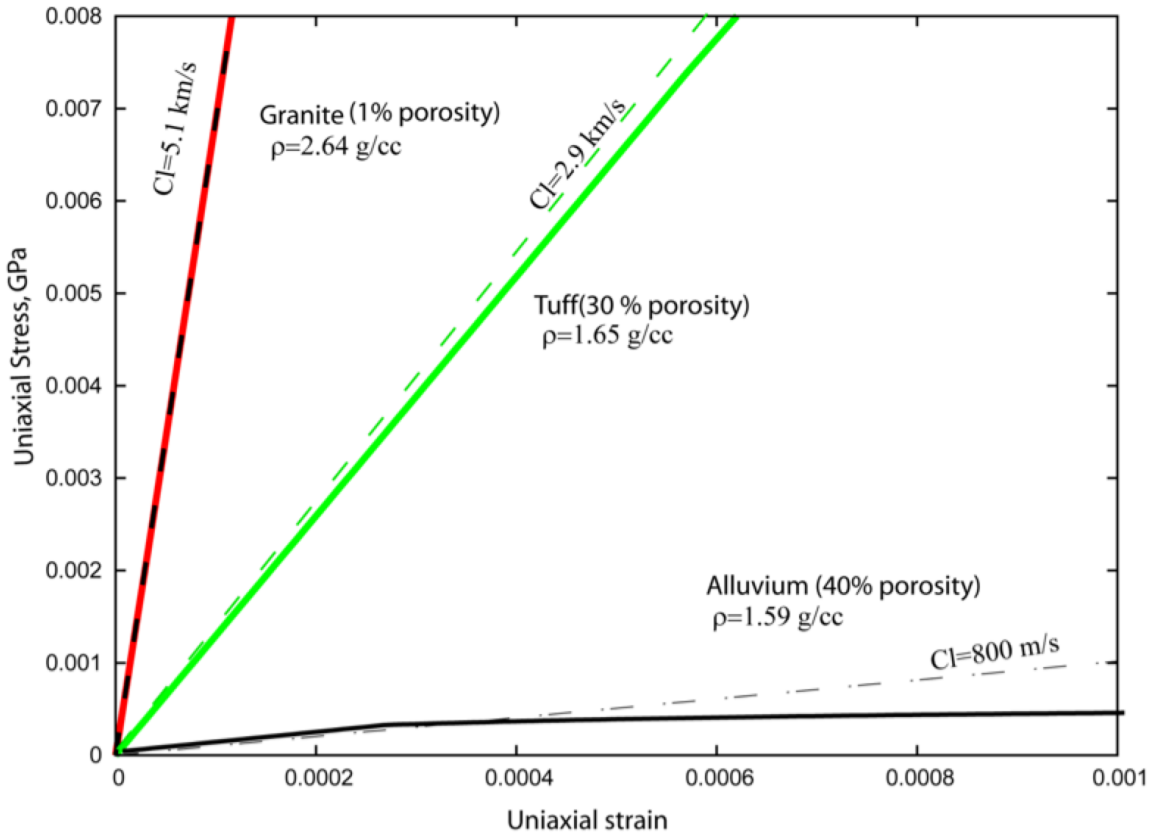

Figure 3. *Uniaxial stress versus uniaxial strain (colored lines) and equivalent elastic (dashed lines) for granite (red), tuff (green) and alluivum (black) material models considered in this study.*

In order to validate simulations of strong-motions excited by explosions we computed motions for a series of explosions of different yield and depth of burial and compared the peak velocities to experimental data from a large compilation of nuclear test data by Perret and Bass (1974). Figure 4 shows the observed (Perret and Bass, 1974) and simulated peak velocity versus scaled range for nuclear explosions in granite, tuff and alluvium. The scaled range is taken as the slant distance divided by the explosive yield to the 1/3 power. Note that the peak velocities are largest for granite, then tuff, then alluvium. While there is scatter in the observation data and the granite data do not span a large range, the simulations provide a reasonably good fit to the experimental data. This gives us confidence that GEODYN simulations and our material models can accurately model near-source motions in the regions of non-linear behavior.

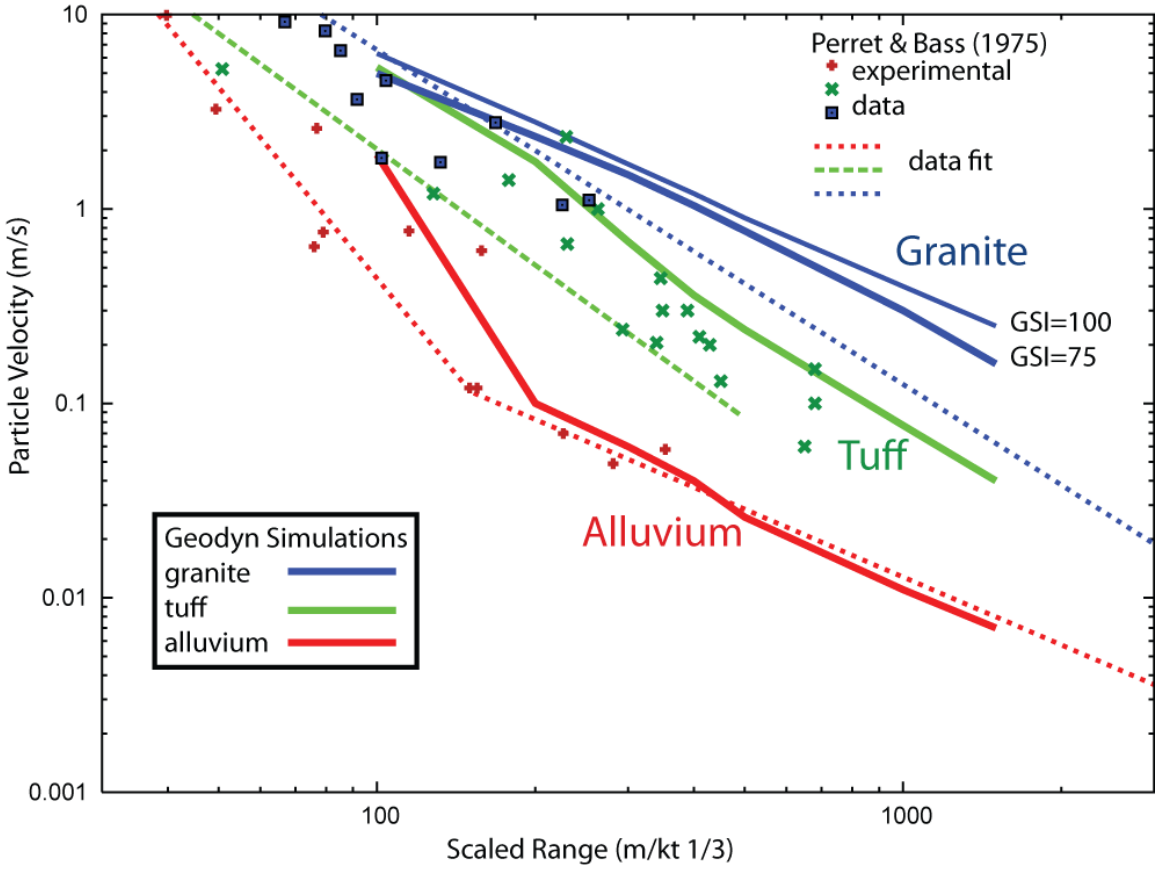

Figure 4. *Observed (points, from Perret and Bass, 1974) and simulated peak velocity versus scaled range for nuclear explosions in granite, tuff and alluvium (shown in blue, green and red, respectively). Peak velocities from GEODYN simulations are shown as solid lines with the same color-coding.*

Parametric Investigations of Seismic Excitation by Underground Explosions

We performed a series of GEODYN simulations to investigate the effects of explosion emplacement conditions on ground motions. The simulations were performed in two-dimensions using a uniform solid material (granite, tuff or alluvium) overlain by air. We sampled the wavefield time-histories at a number of points and decomposed the motions

into radial (P-wave) and vertically polarized transverse (SV-wave) motions. Figure 5 shows the decomposed velocity time-histories at a range of 500 m from the shot point (in the elastic region) at an angle of 60° from the horizontal, corresponding to a near teleseismic take-off angle. P- and SV-wave motions are shown together as colored and black seismograms, respectively. Notice the great difference in the arrival time, pulse duration and P-to-SV energy partitioning for the different materials. The shot in granite results in a fast arriving wave with very sort duration (~0.01 s) while the shot in tuff arrives later with a longer duration (~0.2 s). The shot in alluvium results in much weaker motions (shown amplified by a factor of ten in Figure 5) with more complexity and longer duration than the other materials.

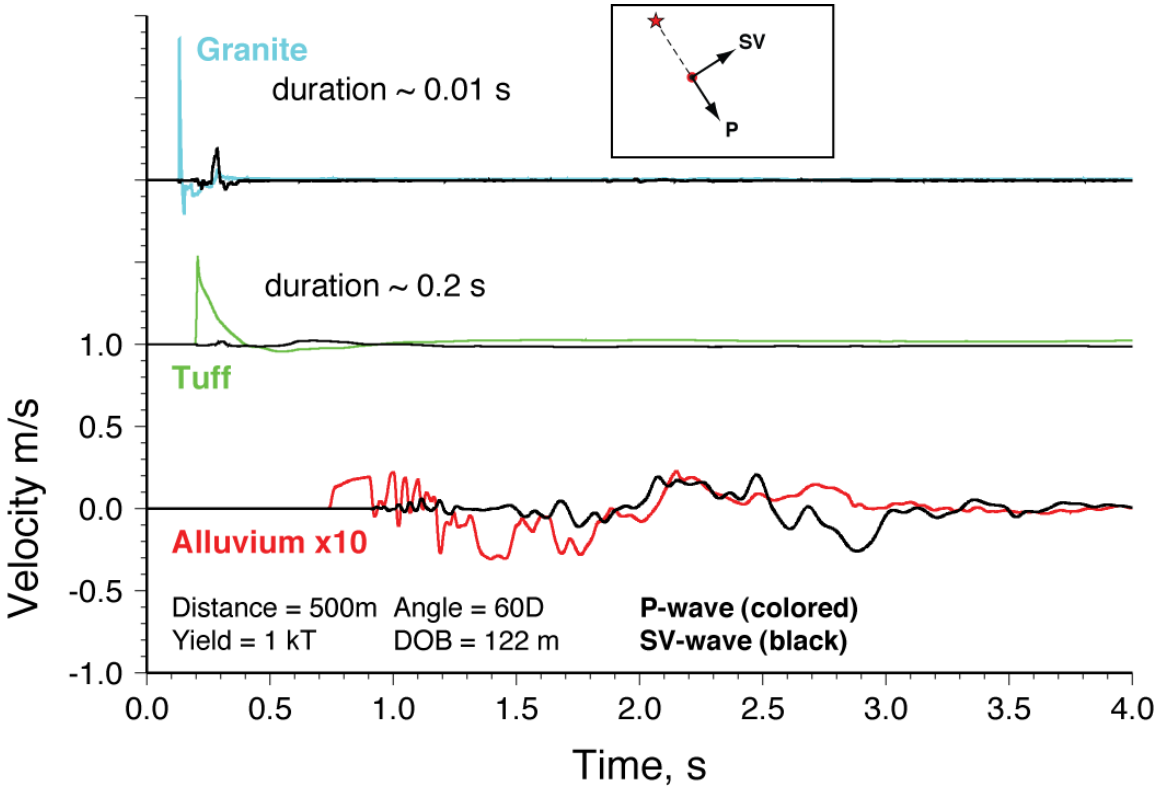

Figure 5. *P-wave velocity time-histories for 1 kT chemical explosions in granite (cyan), tuff (green) and alluvium (red). The corresponding SV-wave time-histories (black) on the same scale as the P-wave motions. Note that motions in alluvium are amplified by a factor of ten. (**inset**) Illustration of the decomposition of motions from a shot point (star) to a marker point (circle) to P (radial) and SV (transverse) motions.*

The differences in P-wave pulse width are also reflected in corner frequencies of amplitude spectra (not shown). Also note the differences in the relative P- and SV-wave amplitudes. The shot in alluvium generates 1 Hz P- and SV-wave energy of roughly equal amplitude. These differences in P- and SV-wave spectral amplitudes result in very different high-frequency P/S amplitude ratios used for event identification. Cross-spectral ratios from Nevada Test Site (NTS) explosions reported by Walter et al. (1995) show different values depending on emplacement conditions, with strong materials have high values and weak materials having low values (Figure 6a). Preliminary results

indicate that the simulated cross-spectral ratios (high-frequency P / low-frequency S) are consistent with these observations (Figure 6b).

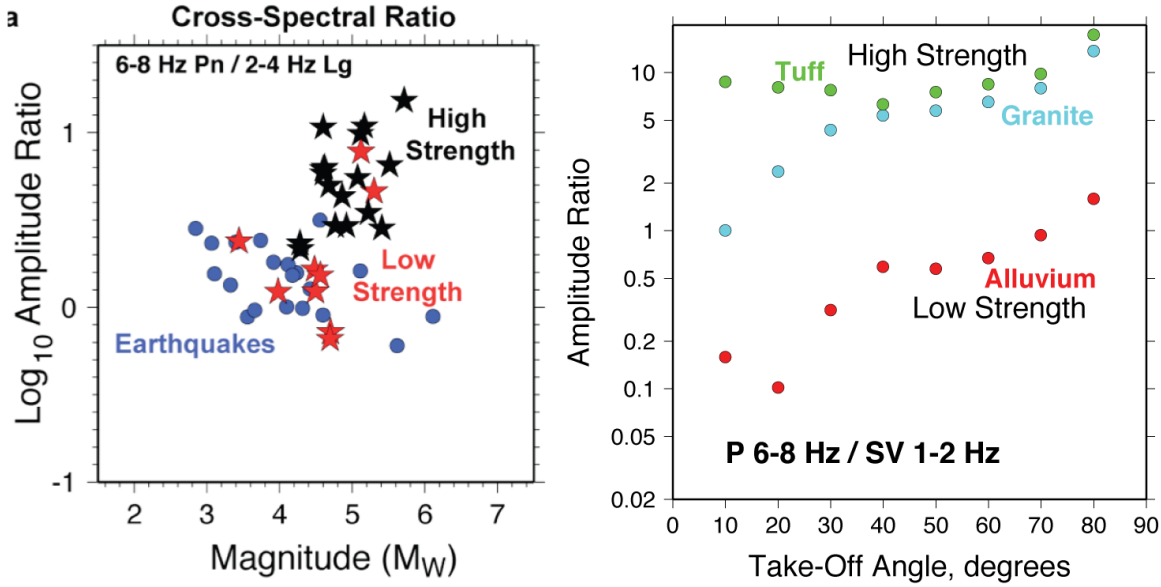

Figure 6. (a, left) *Observed 6-8 Hz Pn/ 2-4 Hz Lg cross-spectral ratios for NTS earthquakes (blue circles) and explosions (stars), with ratios for high and low strength emplacement conditions indicated by black and red stars, respectively.* ***(b, right)*** *6-8 Hz P/1-2 Hz SV cross-spectral ratios versus take-off angle (measured from horizontal) for three material models*

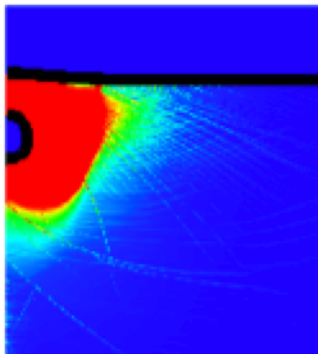

Figure 7. *Post-event strain field for a 1 kT chemical explosion in tuff at a normal scaled depth-of-burial (122 m): the inner circle indicates the cavity; red values indicate strains greater then 10^{-6}; and darkest blue outside the cavity corresponds to elastic motions. The domain shown spans approximately 500 m in each dimension.*

Similar to many other numerical methods for wave propagation, GEODYN allows us to sample the strains and record the strain at all points in the computational domain during the simulation. Figure 7 shows the peak strain around the shot point for a 1 kT chemical shot in tuff at the normal scaled depth-of-burial (122 m). The cavity is formed around the

shot point and indicated by the inner semi-circle. Colors show the strain with red colors corresponding to plastic strains of 10^{-6} or greater and the darkest blue outside the cavity corresponding to elastic strains. Self-affine properties of the material strength cause the asymmetric pattern of strains (yellow to cyan colors) due to fracture.

Note that the shape of the plastic-elastic transition is not spherical, as the idealized explosion source models assume, but rather is elongated at the surface suggesting the free-surface impacts the strain within the rock.

In order to investigate the effect of gravity and demonstrate the importance of lithostatic pressure on cavity size and source pulse duration, we computed the motions for a 1 kiloton explosion in limestone (12% porosity) at various depths of burial (DOB) with and without gravity and lithostatic pressure. Figure 8 shows the resulting radial velocities at a fixed distance from the shot point within the rock (away from the surface). The shock-wave pulse duration and cavity radius (not shown) are insensitive to depth without gravity. However, including gravity and lithostatic pressure result in shorter pulse durations and smaller cavities for deeper explosions. This behavior is consistent with theoretical explosion source models, such as the Mueller and Murphy (1971), Hadley and Helmberger (1981), Burdick et al. (1983) and Saikia et al. (2001).

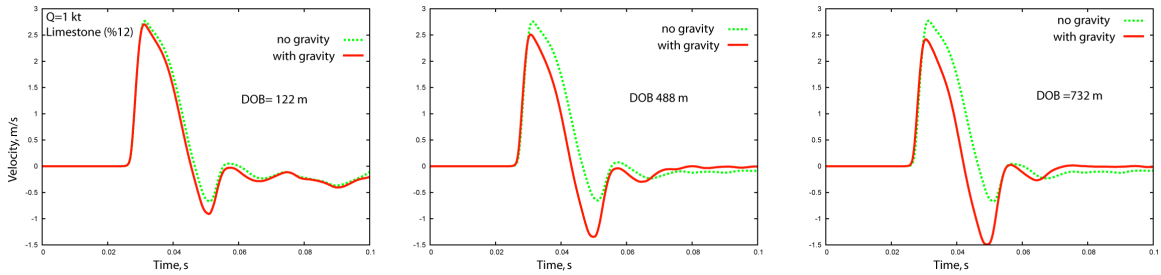

Figure 8. *Radial velocity time-histories at a fixed distance within the solid for 1 kiloton explosion in limestone for three depths of burial (DOB = 122, 488 and 732 m). The velocities with gravity (red) indicate shorted durations for deeper DOB's.*

Similar calculations of a 1 kiloton explosion in granite at different DOB's showing the effect of lithostatic pressure. Figure 9 shows the radial velocity time-histories at 100 m and 300 m for three DOB's.

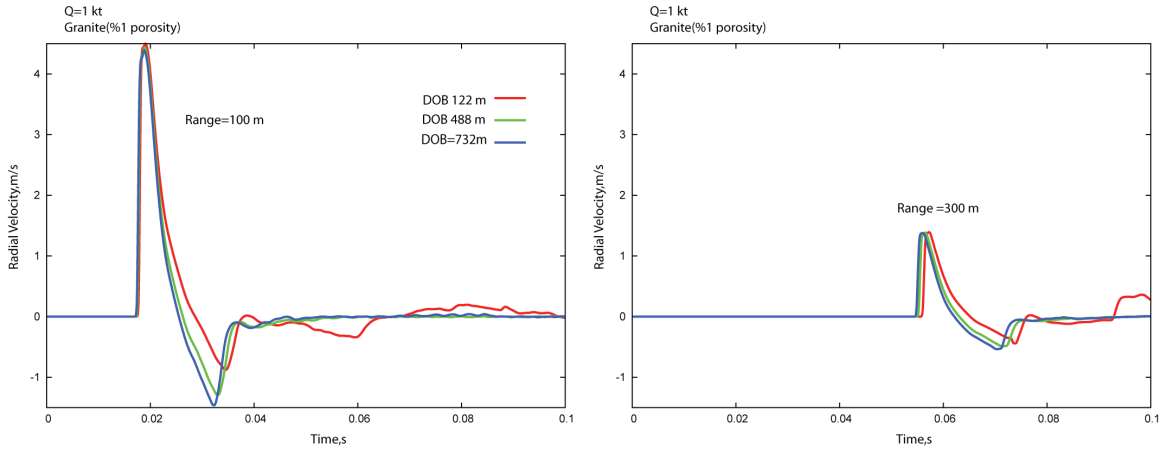

Figure 9. *Radial velocity time-histories at 100 m (left) and 300 m (right) for solid for 1 kiloton explosion in limestone for three depths of burial (DOB = 122, 488 and 732 m).*

Notice that the DOB has virtually no effect on the rise time and amplitude of the initial pressure wave. However, the rarefaction (negative pressure pulse) corresponding to the rebound of the cavity is strongly impacted by the depth and lithostatic pressure with the deeper shot resulting in a stronger more rapid rebound due to the mechanically stronger and denser material at depth. The shorter pulse duration is related to the resulting cavity size.

These results demonstrate that we can compute motions generated by underground explosions in realistic earth materials. Further work on this thrust will focus on tying simulated motions to explosion source models (e.g. Mueller and Murphy, 1971; Helmberger and Handley, 1981; Denny and Johnson, 1991) and experimental data where possible.

Coupling of GEODYN to WPP

In order to simulate seismic ground motions to distances where observations are typically made (> 1 km), we are coupling of motions from GEODYN to our anelastic wave propagation code, WPP. This is a one-way coupling where we compute the response of the material in the non-linear regime through to the elastic regime. GEODYN calculations cover the complete physics of non-linear behavior and are thus computational very expensive. For elastic motions GEODYN is not the most efficient choice of algorithm and such motions are better modeled with WPP. WPP is an anelastic finite difference code for modeling seismic waves in solid materials (Nilsson et al., 2007). WPP includes mesh refinement for increasing the grid spacing as seismic wavespeeds increase with depth and now include free-surface topography (Appelo and Petersson, 2008). Because GEODYN models the rapidly propagating and evolving shock-wave, it works on very small spatial and temporal scales, typically centimeters and microseconds, respectively. WPP can handle a broad range of spatial and temporal scales, but in order to propagate motions to large distances where seismic data might be recorded (e.g. 1-1000 km), the resolution must be reduced so that the problem can be accommodated on the available resource. Typically, we use spatial grid sizes of 1-100 m

to model motions with frequencies below 1-100 Hz. Thus the signals must be filtered to remove high-frequencies that cannot be accurately resolved on the WPP grid. Currently this is done as a pre-processing step performed on the GEODYN output before inputting to WPP.

Early in the project we ran a series of one-dimensional GEODYN calculations to replicate peak displacements from a series of chemical high-explosive (HE) experiments in limestone performed in Kirghizia in 1960 (Murphy et al., 1997). The generic strength model described in Vorobiev (2008) was used in GEODYN to model limestone with 0.5% porosity. In situ experimental measurements of ground motion at different distances from the shot point were reported by Murphy et al. (1997). The explosions and motion recordings reported in this study were conducted in the subsurface in essentially rock whole-space conditions, making them ideal for our simulation validation experiments. Figure 10 shows the peak displacements versus range for two experiments (circles) and comparison of the GEODYN and WPP displacement time-histories for each experiment. GEODYN calculations were carried out beyond the elastic transition (indicated by the vertical dashed lines at 40 m range).

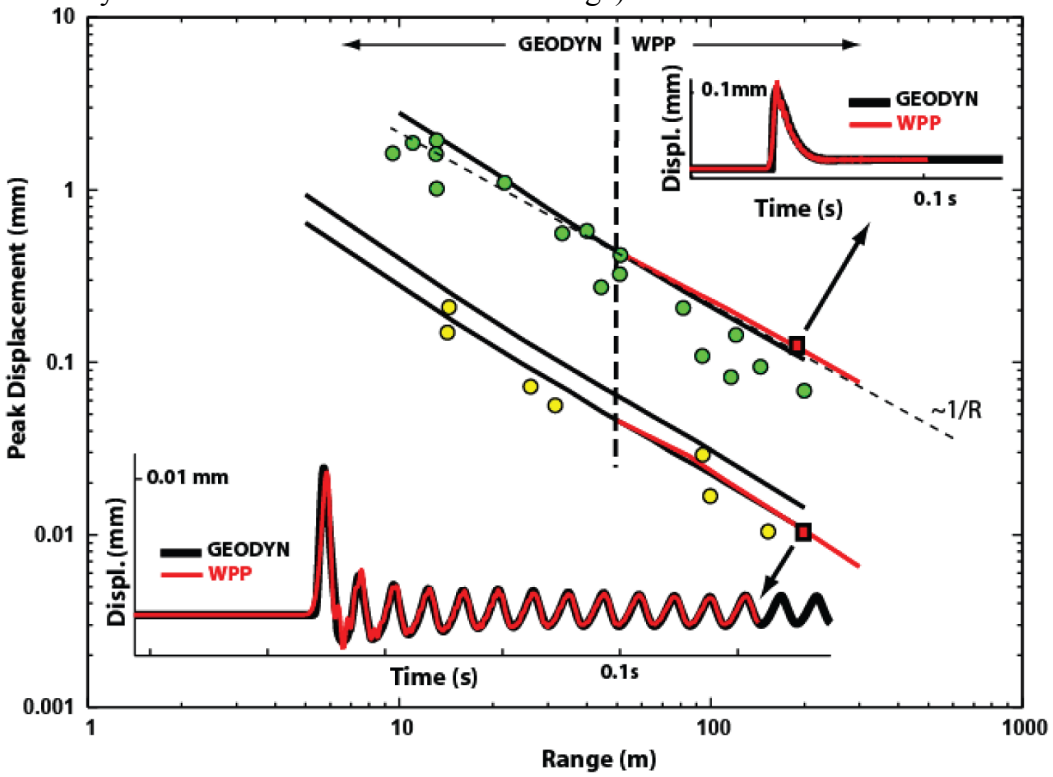

Figure 10. *Peak displacements as a function of range for experimental data (circles) from Murphy et al., (1997) and GEODYN calculations (black line). Also shown are the displacement time-histories (inset plots) from GEODYN (black lines) and from the one-way code coupling approach where motions were passed from GEODYN to WPP (red lines), propagated with both codes and compared at 200 m range (red square).*

In this example we passed the motions from GEODYN to WPP at a distance of 40 m and propagated motions in both codes to 200-300 m. The GEODYN calculation is extended into the linear elastic regime and results indicate that the peak displacements from both

codes match the amplitudes versus range perfectly. Furthermore, the time-histories agree nearly perfectly indicating that numerical artifacts due to interpolation or grid dispersion are minimal. These calculations were valid up to frequencies of 100 Hz.

During the last year significant effort was placed on more sophisticated coupling allowing 2D or 3D GEODYN calculated motions to be passed to WPP in 3D. Motions are saved on a dense grid of points on the faces of a cube and passed to WPP as forcing on an internal surface. In this case the motions from GEODYN are interpolated onto the faces of a cube beyond the plastic-elastic transition region of the explosion. These motions excite elastic motions within the WPP domain and propagate as seismic waves. Figure 11 shows the motions at three locations for both GEODYN and WPP after coupling. The motions were passed at 288 m (left) and propagated with both GEODYN and WPP to farther distances (366 and 488 m). The time-histories agree very well indicating that the GEODYN excitation is introduced correctly and no numerical artifacts bias the calculation.

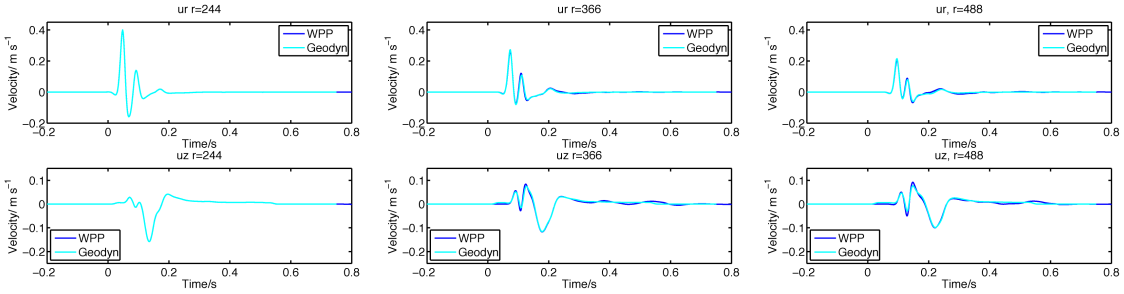

Figure 11. *Radial and vertical velocity time-histories at three locations (244, 366 and 488 m) for GEODYN (cyan) and WPP after coupling (blue). Motions were passed to WPP at 288 m.*

Conclusions

In this last twelve months we have made good progress toward a general capability to compute motions excited by contained underground explosions with GEODYN, a code for modeling shock-waves in earth materials, and pass these motions to WPP for propagating them to large distances. Parametric studies show that GEODYN can reproduce important features of explosion source models. Future will attempt to relate simulation results to explosions source models and compare simulations with available empirical data. The basic capability to pass motions from GEODYN to WPP is established. Future work will focus on testing the numerical accuracy and stability of the one-way coupling, to make sure the coupling is correct and efficient.

Acknowledgements

This work performed under the auspices of the U.S. Department of Energy by Lawrence Livermore National Laboratory under Contract DE-AC52-07NA27344.

References

Aki and Richards (1980). Quantitative seismology, Freeman and Co., New York.

Antoun, T. H., I. N. Lomov and L. A. Glenn (2001). Development and application of a strength and damage model for rock under dynamic loading, proceedings of the 38th U.S. Rock Mechanics Symposium, Rock Mechanics in the National Interest, D. Elsworth, J. Tinucci and K. Heasley (eds.), A. A. Balkema Publishers, Lisse, The Netherlands, 369-374.

Antoun, T. H. and I. N. Lomov (2003). Simulation of a spherical wave experiment in marble using multidirectional damage model, 13th American Physical Society Topical Conference on Shock Compression of Condensed Matter, Portland, OR July 20-25, 2003.

Antoun, T. H., I. N. Lomov and L.A. Glenn (2004). Simulation of the penetration of a sequence of bombs into granitic rock, *Int. J. Impact Eng*., **29**, 81-94.

Appelo, D., and N.A. Petersson, (2008). A stable finite difference method for the elastic wave equation on complex geometries with free surfaces, *Comm. Comput. Phys*., **5**, 84-107.

Helmberger, D. and D. Hadley (1981). Seismic source functions and attenuation form local and teleseismic observations of NTS events JORNADA and HANDLEY, *Bull. Seism. Soc. Am.*, **71**, 51-67.

Lamb, F. K. (1988). Monitoring yields of underground nuclear tests using hydrodynamic methods, *Nuclear Arms Technologies in the 1990s,* D. Schoeer and D. Hafemeister (eds.), AIP Conference Proceedings, New York

Lomov. I. N., T. H. Antoun, J. Wagoner and J. Rambo (2003). Three-dimensional simulation of the Baneberry nuclear event, Proceedings of the 13th American Physical Society Topical Conference on Shock Compression of Condensed Matter, Portland, OR July 20-25, 2003.

Mueller, R. amd J. Murphy (1971). Seismic characteristics f\of underground nuclear detonations Part 1: Seismic source scaling, *Bull. Seism. Soc. Am*., **61**, 1675-1692.

Murphy, J. (1981). P wave coupling of underground explosions in various geologic media, in *Identification of Seismic source – Earthquake or Explosion*, E. S. Husebye and S. Mykkelveit (eds.), p. 201-205.

Murphy, J. (1996). Types of seismic events and their source descriptions, in *Monitoring a Comprehensive Test Ban Treaty,* Kluwer Academic Publishers, The Netherlands

Murphy, J.R., Kitov, I.O., Rimer, N., Adushkin, V.V., Barker, B.W. (1997) Seismic characteristics of cavity decoupled explosion in limestone: An analysis of Soviet high explosive test data. *Journal of Geophysical Research,* **102**(12), 27393-27405.

Nilsson, S., N.A. Petersson, B. Sjogreen, H.-O. Kreiss (2007). Stable difference approximations for the elastic wave equation in second order formulation, *SIAM J. Numer. Anal*., **45**, 1902-1936.

Perret W. R. Bass R. C. (1974). Free-field ground motion induced by underground explosions, Sandia National LaboratoryReport No. SAND74-0252.

Rodean, H (1981). Inelastic prcesses in seismic wave generation by underground explosions, in *Identification of Seismic source – Earthquake or Explosion*, E. S. Husebye and S. Mykkelveit (eds.), p. 97-189.

Rubin, M. B., O. Vorobiev and L. A. Glenn (2000). Mechanical and numerical modeling of a porous elastic-viscoelastic material with tensile failure, *Int. J. Solids and Structure*, **37**, 1841-1871.

Saikia, C., D. Helmberger, R. Stead and B. Woods (2001). Effects of source RDP Models and near-source propagation: Implication for seismic yield estimation, *PAGEOPH*, **158**, 2173-2216.

Sharpe, J. (1942) The production of elastic waves by explosive pressures. I. Theory and empirical field observations, *Geophysics*, **7**, 144.

Vorobiev, O. (2008). Generic strength model for dry jointed rock masses, *Int. J. of Plasticity*, **24**, 2221-2247.

Walter, W., K. Mayeda and H. Patton (1995.). Phase and spectral ratio discrimination between NTS earthquakes and explosions. Part I: Empirical observations, *Bull. Seism. Soc. Am.*, **85**, 1050-1067.

Werth, G. and R. Herst (1963). Comparison of amplitudes of seismic waves from nuclear explosions in four mediums, *J. Geophys. Res*., **68**, 1463-1475.

Table 1. Material properties for the three geologic media considered in this study.

Material	Density (kg/m^3)	Compressional wave speed (m/s)	Shear wave speed (m/s)	Porosity (%)
Alluvium	1590	800	462	40
Tuff	1650	2900	1676	30
Limestone				
Granite	2640	5100	2948	1

GEODYN – Parameteric simulations to perform in support of this paper

Material Models:
Granite, Limestone, Tuff and
2 kinds of alluvium:
one stronger (P-wave velocity say 1500 km/s)
one weaker (P-wave velocity say 800 km/s)
only run stronger material for parametric studies

Yields:
W = 0.2, 0.5, 1, 2, 4 kiloton yields for the granite

DOB:
DOB = 122, 244, 488, 732 m DOB

Total Runs:
4 material models * 5 yields * 4 DOB's = 80 runs

Output

Marker Points (MP's):
We do not need as many was we have been calculating. Try this:

MP's should be along radii from source in quasi-log-distance sampling both the non-linear and linear elastic regions. Radii should be from outside the cavity (>100 m) to well into the elastic zone:
So 100, 200, 400, 800, 1200, 1600 m would OK
We only need a few radial lines, say at 0, 20 40 60 80 degrees from the horizontal
So 0 degrees corresponds to the DOB
Also include MPs at these distances along the surface, can be slant or epicentral distance.
This results in about 6 MP's per line and 6 lines for **36 total MP's**
We may not use the distant marker points for the 80 degree line (it's out of domain)
For MP files output the usual variables, including the plastic strain

Cavity size:
We need to compute the cavity radius for each run, so that we can establish the dependence of cavity size on yield DOB, yield and material.

Plastic Deformation:
It would be good to output images of the plastic deformation at some final time. I can plot these if you can output files with the two-dimensional field values. For the format, binary raster is OK, but I'll need good description and example to test a file to make sure I can read and plot it.